Taylor & Francis
Taylor & Francis Group

Journal of Biomaterials Science, Polymer Edition

ISSN: 0920-5063 (Print) 1568-5624 (Online) Journal homepage: http://www.tandfonline.com/loi/tbsp20

Construction of a PLGA based, targeted siRNA delivery system for treatment of osteoporosis

Deniz Sezlev Bilecen, Jose Carlos Rodriguez-Cabello, Hasan Uludag & Vasif Hasirci

To cite this article: Deniz Sezlev Bilecen, Jose Carlos Rodriguez-Cabello, Hasan Uludag & Vasif Hasirci (2017) Construction of a PLGA based, targeted siRNA delivery system for treatment of osteoporosis, Journal of Biomaterials Science, Polymer Edition, 28:16, 1859-1873, DOI: 10.1080/09205063.2017.1354675

To link to this article: http://dx.doi.org/10.1080/09205063.2017.1354675

Accepted author version posted online: 19 Jul 2017.
Published online: 31 Jul 2017.

Submit your article to this journal

Article views: 36

View related articles

View Crossmark data

Full Terms & Conditions of access and use can be found at
http://www.tandfonline.com/action/journalInformation?journalCode=tbsp20

Download by: [University of Alberta] **Date:** 18 September 2017, At: 13:21

JOURNAL OF BIOMATERIALS SCIENCE, POLYMER EDITION, 2017
VOL. 28, NO. 16, 1859–1873
https://doi.org/10.1080/09205063.2017.1354675

Taylor & Francis
Taylor & Francis Group

Check for updates

Construction of a PLGA based, targeted siRNA delivery system for treatment of osteoporosis

Deniz Sezlev Bilecen[a,e], Jose Carlos Rodriguez-Cabello[b], Hasan Uludag[c] and Vasif Hasirci[a,d,e]

[a]BIOMATEN, Middle East Technical University (METU), Center of Excellence in Biomaterials and Tissue Engineering, Ankara, Turkey; [b]G.I.R. Bioforge, University of Valladolid, CIBER-BBN, Valladolid, Spain; [c]Department of Chemical and Materials Engineering, University of Alberta, Edmonton, Canada; [d]Department of Biological Sciences, METU, Ankara, Turkey; [e]Department of Biotechnology, METU, Ankara, Turkey

ABSTRACT

Osteoporosis, a systemic skeletal disorder, occurs when bone turnover balance is disrupted. With the identification of the genes involved in the pathogenesis of the disease, studies on development of new treatments has intensified. Short interfering RNA (siRNA) is used to knockdown disease related gene expressions. Targeting siRNA *in vivo* is challenging. The maintenance of therapeutic plasma level is hampered by clearance of siRNA from the body. Targeted systems are useful in increasing the drug concentration at the target site and decreasing side effects. Aim of the present study was to develop an injectable siRNA delivery system to protect siRNA during systemic distribution and target the siRNA to bone tissue using a thermoresponsive, genetically engineered, elastin-like recombinamer (ELR), designed to interact with the mineral component of bone. The delivery system consisted of DNAoligo as a siRNA substitute complexed with the cationic polymer, polyethyleneimine (PEI), at N/P ratio of 20. The complex was encapsulated in poly(lactic acid-co-glycolic acid) (PLGA) nanocapsules. PLGA capsules were characterized by SEM, TEM and XPS. FTIR was used to show the preferential attachment of ELR to HAp. Encapsulation efficiency of the complex in PLGA nanocapsules was 48%. The release kinetics of the complex fits the Higuchi release kinetics.

ARTICLE HISTORY
Received 17 April 2017
Accepted 10 July 2017

KEYWORDS
PLGA; nanocapsules; siRNA; targeted delivery; osteoporosis

Downloaded by [University of Alberta] at 13:21 18 September 2017

1. Introduction

Osteoporosis is a systemic disease characterized by increased bone resorption relative to formation which eventually leads to reduced bone mineral density (BMD), bone mass and strength [1]. This structural failure of the skeleton causes 8.9 million fractures worldwide [2], some leading to mortality [3]. Pharmacological agents used for the treatment of the disease either suppress bone resorption (bisphosphonates, denosumab, calcitonin and selective estrogen receptor modulators) or have anabolic effects on bone formation (parathyroid hormone) [4]. The currently used treatment strategies have

CONTACT Vasif Hasirci vhasirci@metu.edu.tr

© 2017 Informa UK Limited, trading as Taylor & Francis Group

limitations as low bioavailability, gastric problems and long term safety concerns [5–7]. These drawbacks caused an urgency in delivering these drugs in formulations where bioavailability and patient compliance are increased. To address these issues, attention is now being focused on delivering the drugs with carrier systems such as synthetic and organic nanoparticles, liposomes or CaP cements [6,8]. Application of drugs using carrier systems elicits advantages such as protecting the drug from degradation and reducing toxicity. Besides, since it is applied with the carrier system, biodistribution of the drug becomes partially independent of its own physicochemical properties. A number of studies aiming to increase the bioavailability of conventional drugs using such drug delivery systems has been published [9–12].

In the recent years, due to the various studies that shed light on molecular pathways involved in bone pathology, new molecular targets have been identified to be used in the treatment of bone diseases. RNA interference (RNAi) approach possesses significant therapeutic potential and employs small interfering RNAs (siRNA) to silence any disease-causing gene expression. The employment of RNAi mechanism as a therapeutic tool uses highly sequence-specific gene silencing capability and silence any abnormal expression of disease related genes [13]. The use of RNAi together with biomaterials is becoming a promising approach for the treatment of bone related diseases such as osteoporosis [14]. Studies concerning the treatment of osteoporosis by using siRNA as a therapeutic agent employ *in vitro* administration [15–17] or local delivery of siRNAs [18,19]. Delivering siRNA to bone tissue *in vivo* for the treatment of osteoporosis, however, is very challenging [14,20] due to the high molecular weight, negative charge and instability of the siRNA. In addition to rapid clearance from reticuloendothelial system (RES), premature degradation of siRNA by serum endonucleases, tissue and cell penetration and endosomal escape [21] should be overcome. Due to these challenges, many strategies are now being developed to deliver the siRNA in such delivery systems that siRNA is protected in both extracellular and intracellular environments [22–25].

Branched polyethyleneimine (bPEI) is a cationic polymer that is widely used as a carrier and a protector of siRNA in the delivery to cells. At the physiological pH and under more acidic compartments of cell (endosomes/lysosomes), PEI is highly effective in complex formation with DNA or dsRNA molecules which are polyanionic [26]. This complex protects the siRNA from extracellular nucleases and neutralizes the negative charge of the siRNA which would otherwise impair its cellular uptake. PEI is also known to exert proton sponge effect, which ruptures the endosomal vesicles due to osmotic swelling and high ion influx due to the positive charge it carries [27]. Despite its high efficiency as a gene delivery vehicle, PEI exhibits high cytotoxicity by inducing apoptosis in transfected cells in a concentration and time dependent manner [28]. One of the strategies to reduce the PEI induced toxicity is the encapsulation of PEI in nontoxic carriers [29]. Poly(lactic acid-co-glycolic acid) is a copolymer of lactic acid and glycolic acid; it is a FDA approved, biocompatible and biodegradable polymer that has frequently been used in drug delivery studies [30–33] and in the delivery of nucleic acids [34,35]. PLGA is especially advantageous in siRNA delivery applications because PLGA can be internalized by the cells and escape from endosomes, therefore, accumulate and release its content in the cytoplasm [36] where the released siRNA could function. It is known that a portion of PLGA is exocytosed, however, the internalized nanoparticles that has escaped from the endosomes into the cytoplasm and could act as drug depots and release their contents in

Downloaded by [University of Alberta] at 13:21 18 September 2017

a sustained manner [37]. The release rate of therapeutic agent from PLGA nanoparticles can be controlled by changing the ratio of lactic acid to glycolic acid polymers because the composition affects the crystallinity, hydrophobicity, and as a result, the degradation rate of the polymer [38].

Delivery systems the surfaces of which are modified with specific molecules can increase the drug concentration at the targeted sites [39]. Some of the targeting moieties used for targeting the bone tissue are bisphosphonates [40], tetracyclines [41] or biological molecules such as RGD peptides [42]. In the present study, a genetically engineered polypeptide, Elastin-Like Recombinamer (ELR) was used for this purpose. The specific ELR used in this study contains an osteoconductive sequence which has high affinity for the calcium phosphate crystals in the extracellular matrix of bone tissue [43,44]. This polypeptide was attached onto the PLGA nanocapsule surfaces to target the bioactive agent to the bone tissue.

In this study we have developed an injectable siRNA delivery system targeted to the bone minerals for use in the treatment of osteoporosis. A DNAoligo was used to mimic the siRNA and was complexed with PEI to neutralize the negative charge of the nucleic acid and to attach to the negatively charged cellular components after it is released from PLGA nanocapsules. PLGA nanocapsules loaded with PEI:DNAoligo were coated with ELR to target the nanocapsules to the extracellular matrix of bone tissue. Release behavior of the complex from the PLGA nanocapsules was studied. The schematic representation of the delivery system is illustrated in Figure 1.

Downloaded by [University of Alberta] at 13:21 18 September 2017

2. Materials & methods

2.1. Materials

Poly(lactic acid-co-glycolic acid) (PLGA) (50:50) was purchased from Corbion Purac Biomaterials (Netherlands). Branched PEI (25 KDa) was from Sigma (Germany). ELR (31,877 kDa), was synthesized in the lab of Prof. Rodriguez-Cabello, University of Valladolid (Spain). The Inverse Temperature Transition (ITT) of ELR sequence was around 34 °C, and its amino acid sequence was $[(VPGIG)_2\ (VPGKG)\ (VPGIG)_2]_2$ DDDEEKFLRRIGRFG $[(VPGIG)_2\ (VPGKG)\ (VPGIG)_2]_2$ [43]. Hydroxyapatite (HAp) and polyvinylalcohol (PVA) were purchased from Sigma (Germany) and the crosslinker genipin was from Wako Chemicals (USA). The DNAoligo used as a substitute for the siRNA molecule (sense 5′-GCAGTAGTCTAAGTGGAAATT-3′), and the (antisense 5′-TTTCCACTTAGACTACTGCAA) was purchased from Sentegen (Turkey). The duplex was obtained by annealing the sense and antisense sequences.

2.2. Methods

2.2.1. Preparation and study of PEI:nucleic acid complexes

In order to determine whether the DNAoligo can serve as a substitute for siRNA, complex formation of DNAoligo (and siRNA) with PEI were studied by agarose gel electrophoresis. For this purpose, PEI:nucleic acid complexes with varying nitrogen-to-phosphate ratios (N/P) were prepared in 1X Tris-EDTA (TE) buffer, pH 7.4. For complex formation, DNAoligo (10 μM, 2 μL) and siRNA (10 μM, 2 μL) were mixed with aqueous PEI solutions

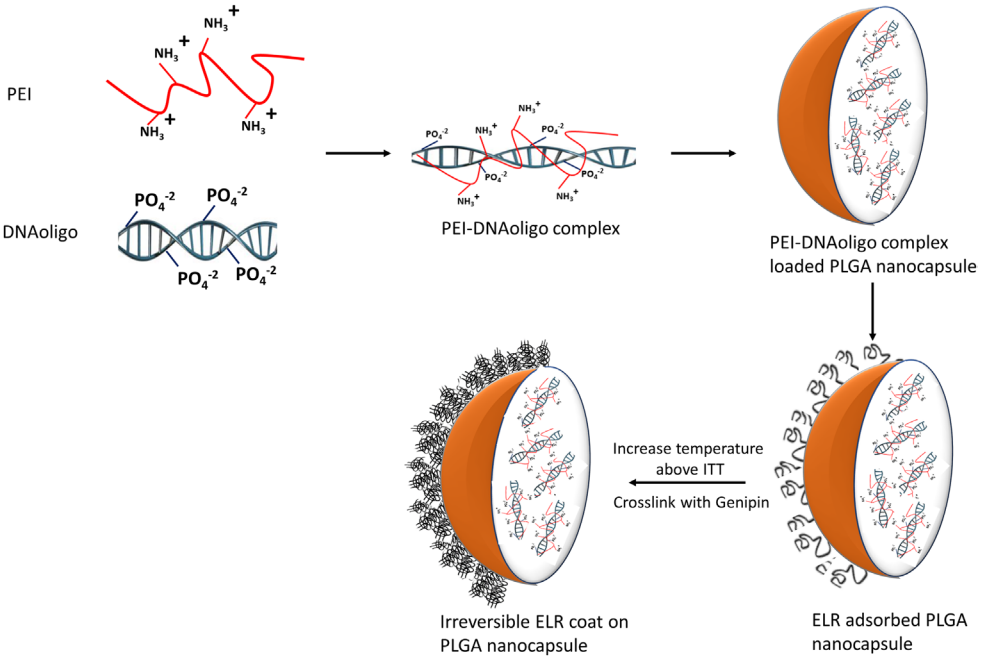

Figure 1. Schematic representation of the delivery system. PEI: Polyethyleneimine; DNA: Deoxyribonucleic acid; PLGA: Poly(lactic acid-co-glycolic acid); ELR: Elastin-like recombinamer; T_t: Temperature transition.

(starting PEI solution concentration was 175 ng/μL) to yield final N/P atomic ratios of 1, 2, 3, 4, 5, 6 and 10. The mixtures were incubated for 20 min at room temperature for complex formation and subjected to agarose gel electrophoresis (2.5%, 100 V, 20 min) and visualized under UV light (UVP GelDoc Imaging System, USA).

2.2.2. Zeta potential of PEI:DNAoligo complexes

The zeta potential of PEI:DNAoligo complexes with varying N/P atomic ratios (0–20) were measured. DNAoligo (10 μM, 6 μL, in TE buffer pH 7.4) was mixed with aqueous PEI solutions (6 μL) to form complexes with N/P ratios of 0, 1, 2, 3, 4, 5, 6, 10 and 20. The mixtures were incubated for 20 min at room temperature and diluted in nuclease-free dH_2O water. The zeta potential of the complexes was measured by Zeta Sizer (Malvern Nano ZS90, UK).

2.2.3. Determination of affinity of the ELR towards hydroxyapatite with Fourier Transform Infrared (FTIR) spectroscopy

ELR affinity to HAp was studied with FTIR-ATR spectroscopy. Disks of HAp crystal (diameter 13 mm) were prepared by compression, an aqueous solution of ELR (5%, 50 μL) was added onto the HAp disk and allowed to dry for 1 h at 25 °C. The HAp disk was washed three times with dH_2O (3 mL) and air dried. As a blank, a HAp disk was produced as reported above, then wetted with dH_2O (50 μL) and air dried before FTIR. As a control of protein adhesion, a HAp disk was treated with aqueous BSA solution (5%, 50 μL) and air dried before FTIR analysis. The FTIR of the samples were obtained in the range 4000–400 cm^{-1} using a FTIR spectrophotometer (PerkinElmer, PIKE GladiATR, USA).

Downloaded by [University of Alberta] at 13:21 18 September 2017

Downloaded by [University of Alberta] at 13:21 18 September 2017

2.2.4. Preparation of PLGA nanocapsules loaded with PEI:DNAoligo complex

Nanocapsules were prepared by water/oil/water ($w_1/o/w_2$) double emulsion method, as previously described, with minor changes [45]. Briefly, PEI:DNAoligo complex (150 µL) was added to PLGA solution (50 mg in 0.5 mL DCM) and probe sonicated on ice for 30 s at 50 W. The resultant emulsion was added into an aqueous PVA solution (3 mL, 4%) and sonicated. The double emulsion was added into another PVA solution (7.5 mL, 0.3%) to increase the aqueous volume and mixed vigorously for 3 h with a magnetic stirrer at room temperature to evaporate DCM. The suspension was centrifuged (18,000 rpm, 10 min, RT) to recover the nanocapsules. The pellet was washed twice with nuclease free dH_2O (3 mL). Nanocapsules were resuspended in nuclease free dH_2O (5 mL), frozen at −20 °C and lyophilized for 8 h under vacuum.

2.2.5. Preparation of ELR coated PLGA nanocapsules

For the coating of PLGA nanocapsules with ELR, inverse temperature transition (ITT) property of the polypeptide was used. Due to ITT, the solubility of ELR decreases above the transition temperature (T_t) causing the aggregation of the recombinamer [46]. The ELR used in this study has a T_t around 34 °C [43]. ELR was dissolved in PBS (1 mL, 10 mg/mL), and PLGA nanocapsules (10 mg) were added. This suspension was incubated at 25 °C in a sonication bath for 1 h and was transferred into 9 mL PBS solution. The suspension was incubated at 37 °C for 20 min followed by centrifugation (13,000 rpm, 10 min, 37 °C). The pellet was resuspended in 10 mL PBS at 37 °C to which genipin solution (1 mL, 10 mg/mL) was added to crosslink the ELR coat on the nanocapsules. The suspension was maintained at 37 °C for 6 h, centrifuged (13,000 rpm, 10 min, 25 °C) and washed.

2.2.6. Nanocapsule characterization

2.2.6.1. Nanocapsule topography with scanning electron microscopy. PLGA nanocapsule suspensions were added on carbon tapes, attached to scanning electron microscopy (SEM) stubs and coated with Au–Pd before imaging using Quanta 400F Field Emission SEM, Netherland.

2.2.6.2. Detection of ELR on nanocapsules with transmission electron microscopy. PLGA nanocapsules were suspended in ethanol and air dried on transmission electron microscopy (TEM) grids. Images were obtained by FEI Technai G2 Spirit Biotwin (USA).

2.2.6.3. X-ray photoelectron spectroscopy. Lyophilized nanocapsules were analyzed with X-ray photoelectron spectroscopy (XPS) (PHI 5000 VersaProbe, USA) for the presence of nitrogen atom as an indicator of the ELR coating.

2.2.7. Particle size distribution

Size distribution of the PLGA nanocapsules were determined using a suspension of PLGA nanocapsules in dH_2O (ca. 1 mg PLGA/5 mL) with Zeta Sizer (Malvern Nano ZS90, UK). For each sample, 3 measurements were performed, 12 runs each, in order to obtain the final size.

Downloaded by [University of Alberta] at 13:21 18 September 2017

2.2.8. Loading and encapsulation efficiency of PEI:DNAoligo in PLGA nanocapsules

The amount of PEI:DNAoligo complex entrapped within the PLGA nanocapsules was determined using the fluorescence intensity (FI) of FAM labelled DNAoligo. A calibration curve was constructed with empty nanocapsules (1 mg) that were suspended in 1X TE buffer and mixed with PEI:FAM labelled DNAoligo complexes (N/P 20) carrying 0.1, 0.2, 0.4, 0.6, 0.8 μg FAM labelled DNAoligo. The FI of the FAM labelled DNAoligo in those suspensions were measured with a spectrofluorimeter (λ_{ex}: 494 nm, λ_{em}: 524 nm) (SpectraMax M2e, Molecular Devices, USA). PLGA nanocapsules (1 mg), prepared using 20 μg DNAoligo (N/P 20), were suspended in 1X TE buffer (200 μL). The amount of complex encapsulated in the nanocapsules was calculated from the calibration curve. The loading and encapsulation efficiency was calculated using the following equations:

$$\text{Loading} = \frac{\text{The amount of encapsulated complex (ng)}}{\text{Amount of nanocapsule (mg)}}$$

$$\text{E.E. (\%)} = \frac{\text{The amount of encapsulated complex (ng)}}{\text{Input amount of complex (ng)}}$$

2.2.9. In situ release of PEI:DNAoligo complex from the PLGA nanocapsules

In order to study the release of the complex, PEI:FAM-labelled DNAoligo (N/P 20)-loaded PLGA nanocapsules (1 mg) were suspended in TE buffer (200 μL) in an Eppendorf tube and kept at 37 °C under constant shaking for 15 days. On Days 1, 3, 5, 7, 10 and 15, suspensions were centrifuged (18,000 g, 20 min). The pellet was resuspended in fresh TE buffer (200 μL) and the FI was measured by using a spectrofluorimeter (λ_{ex} 494 nm, λ_{em} 524 nm) (SpectraMax M2e, Molecular Devices, USA). The amount of complex remained in the capsules was calculated by using FI obtained from the nanocapsules at each time point. The data is presented as 'cumulative complex released vs. time' and treated according to Higuchi equation $\left(\frac{[M]_t}{[M]_\infty} \text{vs.} t^{1/2}\right)$ [47].

3. Results and discussion

3.1. Zeta potential of PEI:DNAoligo complexes

Zeta potential is a function of surface charge of a particle in solution as well as the pH and ionic strength of the test solution [48]. The nucleic acids have negative charges due to the phosphate groups and PEI is positively charged. When they interact, they neutralize each other. Zeta potentials of the PEI:DNAoligo complexes with N/P ratios of 0–20 are presented in Figure 2. Up to the N/P ratio of 5, the zeta potential of the complexes was negative. After that point, where the PEI amount is much higher than the nucleic acids, the zeta potentials of the complexes became positive. These results are in agreement with the literature. Wagner et al., studied the complexation and zeta potentials of PEI:siRNA complexes PEI molecules [49]. In that study, it was also found that increasing the N/P ratios lead to a shift of surface charge from negative to positive. From these results it may be concluded that N/P ratio of 5 is needed to bring the zeta potential of the complexes to −0.4 mV. As the PEI proportion

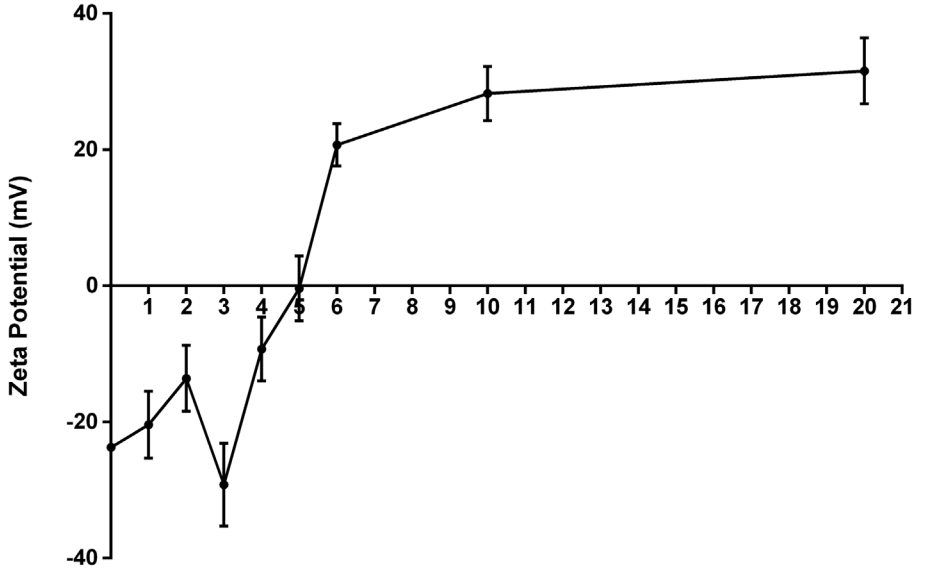

Figure 2. Zeta potential of PEI:DNAoligo complexes with varying N/P ratios. Complexes with up to a N/P ratio of 5 presented negative zeta potentials. The potential shifted to positive values after N/P 5 indicating that all the DNAoligo was in a complex form with PEI.

increased further, the zeta potential became more positive and reached a plateau after a N/P ratio of 10.

3.2. Complexation of PEI with DNAoligo and siRNA

Complexes of PEI:DNAoligo and PEI:siRNA were prepared and compared with agarose gel electrophoresis to determine whether DNAoligo can be used as a substitute for siRNA. Complexes of PEI and nucleic acids are formed as a result of ionic interactions between positively charged nitrogens in PEI and negatively charged phosphates of nucleic acids (Figure 3). These interactions cause the neutralization of the charges and lead to reduced electrophoretic migration in agarose gel during electrophoresis.

Figure 4 shows the migration patterns of PEI:siRNA (Figure 4(A)) and PEI:DNAoligo complexes with N/P ratios of 0–10 on EtBr stained agarose gel (2%) (Figure 4(B)). With N/P ratios of up to 4, nucleic acids were seen to migrate fully which indicates the presence of the uncomplexed form of the nucleic acids. As the N/P ratio increased, the band intensity became weaker. When the N/P ratio was higher than 5, no electrophoretic movement was observed indicating that all the nucleic acid molecules were complexed with PEI and neutralized so their migration was prevented. Since both complexes exhibited the same pattern of complexation, we concluded that the DNA oligo could be used as a substitute for siRNA in the optimization of release studies.

3.3. Affinity of ELR towards hydroxyapatite

In order to check whether ELR could serve as a targeting agent for the PLGA nanocapsules towards bone tissue, the interaction of ELR with calcium phosphate was studied with HAp

Downloaded by [University of Alberta] at 13:21 18 September 2017

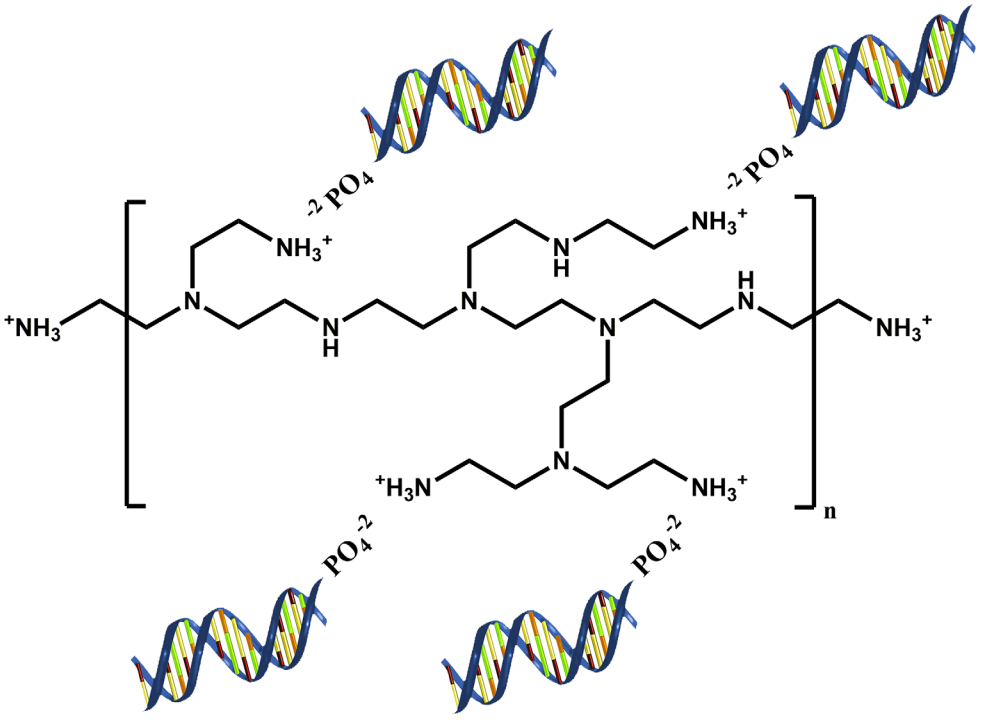

Figure 3. Schematic presentation of PEI:DNAoligo complex. The complexes are formed by the ionic interaction of the positive charged amino groups of PEI ($-NH_3^+$) and negative charged phosphates in the DNAoligo ($-PO_4^{-2}$).

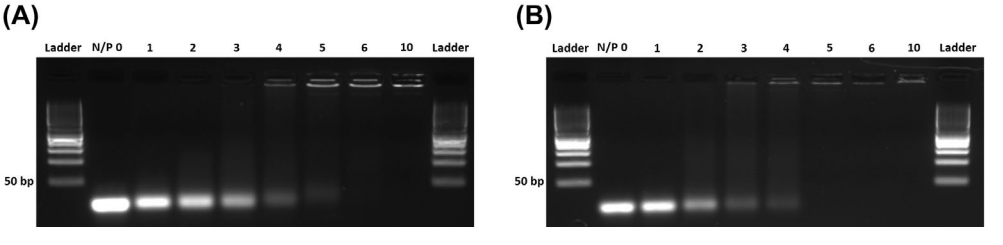

Figure 4. Agarose gel electrophoresis of PEI:nucleic acid complexes. (A) PEI:siRNA, and (B) PEI:DNAoligo complexes with N/P ratios of 0–10. The agarose gel (2.5%) was run for 20 min at 100 V. Above a N/P ratio of 5, nucleic acid migration stopped due to charge neutralization by PEI.

disks using FTIR. The characteristic protein band amide I arises from the vibrational energy of C=O stretching (1600–1700 cm^{-1}) while amide II is a result of N–H bending and C–N stretching [50,51]. In Figure 5, the IR spectrum of ELR adsorbed HAp is presented. As can be seen from the figure, both the amide I (1650 cm^{-1}, C=O bond) and amide II (1534 cm^{-1}, N–H bond) bands are visible in the spectrum of HAp pellet that has adsorbed the ELR.

The binding of ELR and BSA on HAp was compared by using the intensities of amide peaks on HAp. The phosphate $(PO_4)^{-3}$ group peak intensity (1014 cm^{-1}, P–O) [52] obtained from HAp was used as a reference to calculate the peak intensity ratios of amides I and II and phosphate. The peak height ratios of the amide I and amine II to phosphate are presented in

Downloaded by [University of Alberta] at 13:21 18 September 2017

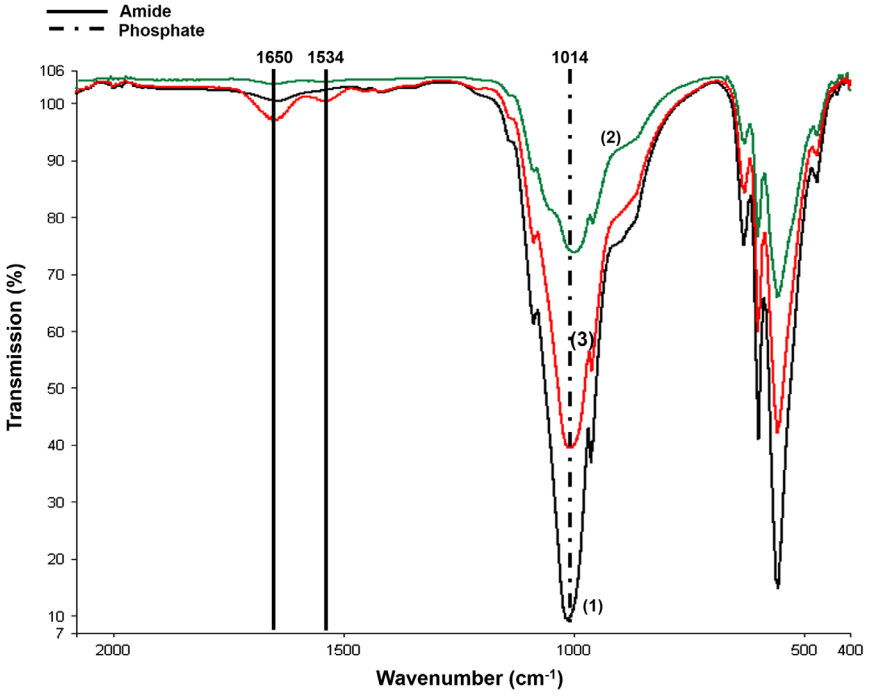

Figure 5. FTIR-ATR spectra of HAp and polypeptide interaction. (1) HAp, (2) BSA adsorbed HAp, and (3) ELR adsorbed HAp pellet. Amide I and II bands are visible in the FTIR spectrum of ELR and BSA adsorbed HAp indicating that both proteins were adsorbed on HAp pellets.

Table 1. For HAp-ELR, the NH-to-PO ratio (2.9×10^{-2}) is higher than that with HAp-BSA (1.8×10^{-2}) (Table 1). Similarly, the CO-to-PO ratio is much higher on ELR treated HAp. These suggest that there is more protein on HAp when ELR is used and might imply that ELR has a higher affinity towards HAp than BSA. Based on these results, it was concluded that ELR could be used as a molecule to target the PLGA nanocapsules to HAp crystals present in the structure of the bone.

3.4. Topography of PLGA nanocapsules

The morphology of the nanocapsules was studied with SEM (Figure 6). Uncloated PLGA nanoparticles appeared as smooth and spherical (Figure 6(A)), however, coated nanoparticles had rough surfaces and we interpreted this roughness to be due to the presence of protein (ELR) coat (Figure 6(B)).

3.5. Detection of ELR on nanocapsules with TEM and XPS

After observing the rough surface of ELR coated PLGA nanocapsules in SEM micrographs, the capsules were studied with TEM to show the protein coat on the surface of nanocapsules (Figure 7).

Downloaded by [University of Alberta] at 13:21 18 September 2017

Table 1. FTIR peak intensity ratios (C=O/P–O) and (N–H/P–O).

FTIR peak intensity ratios	C=O/P–O	N–H/P–O
HAp	1.7×10^{-2}	–
HAp-BSA	3.2×10^{-2}	1.8×10^{-2}
HAp-ELR	8.4×10^{-2}	2.9×10^{-2}

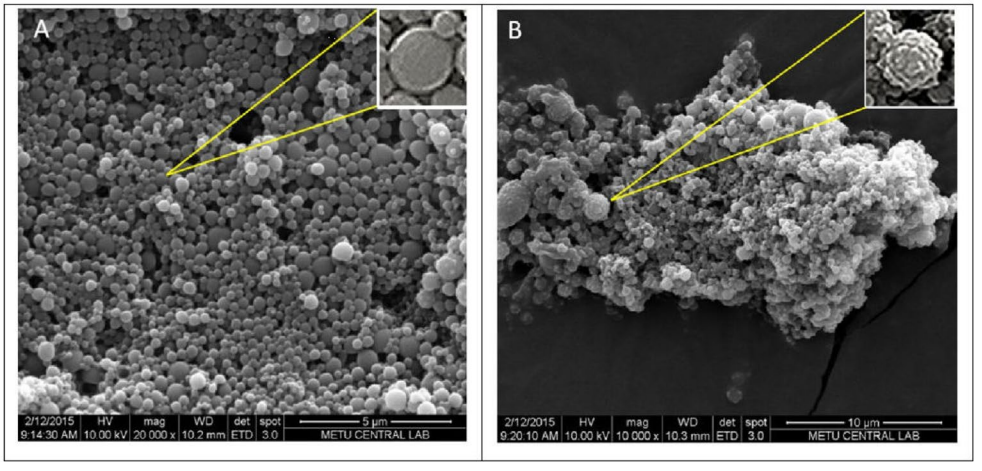

Figure 6. SEM of PLGA nanocapsules. (A) Uncoated, (B) ELR coated. The rough surface of ELR coated PLGA nanocapsule implies the presence of the protein coat on the capsules.

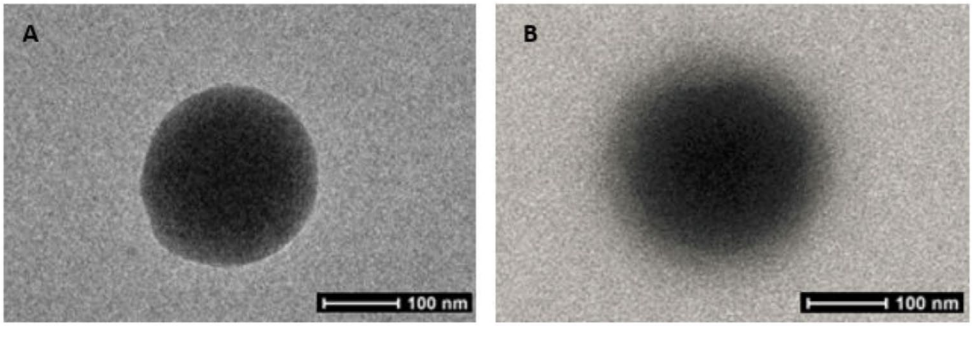

Figure 7. TEM micrographs of PLGA nanocapsules. (A) Uncoated, (B) ELR coated. The fuzzy appearance of the edges of ELR coated PLGA nanocapsule implies the ELR on the surface.

In Figure 7(B), a halo which we interpreted as the protein coat on the surface of nanocapsules is visible while in Figure 7(A), the uncoated PLGA nanocapsule appears with a crisp outline.

Uncoated and ELR coated PLGA nanoparticles were also analyzed with XPS for nitrogen atom as an indicator of protein (ELR) presence on the PLGA nanocapsules [53]. XPS results of the coated sample (Figure 8(B)) indicate the presence of a significant amount of nitrogen atom (11.7%) on the sample while no nitrogen could be detected on the uncoated sample (Figure 8(A)). Since the source of this nitrogen can only be the ELR treatment, the presence of the ELR coat on the PLGA nanocapsules was confirmed.

Downloaded by [University of Alberta] at 13:21 18 September 2017

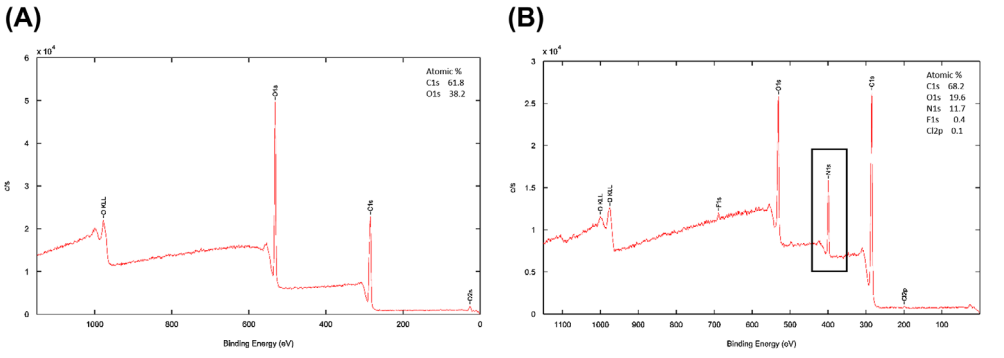

Figure 8. XPS spectra of PLGA nanocapsules. (A) Uncoated, (B) ELR coated. The XPS spectra of the capsules show the presence of nitrogen in the ELR coated PLGA nanocapsules.

Downloaded by [University of Alberta] at 13:21 18 September 2017

3.6. Particle size distribution

The size of a drug delivery particle is always important in its transport across membranes and through the tissues. It is therefore important in the delivery of the system developed in this study, too. The average diameter of uncoated, empty PLGA nanocapsules (main peak representing 100% of the particles) was determined to be 208 ± 83 nm (Table 2). Loading of PEI:DNAoligo into the capsules and binding of ELR over the capsule did not change the diameter of the capsules (197 ± 76 and 220 ± 81) (Table 2). Polydispersity index (PDI) is the measure of particle size distribution and values between 0.17 and 0.63 obtained in this study represent mid-range size distribution and these particles are suitable for use in delivery study.

One of the parameters that affect the transport and extravasation of nanoparticles through the endothelium of blood capillaries is the diameter of the nanoparticles. The endothelium of bone marrow has discontinuous fenestrations with a size range of 100–200 nm [54]. Fifty-three percent of the loaded PLGA nanocapsules with ELR coat obtained in this study had a diameter of less than 200 nm. The high fraction of nanoparticles with sizes lower than 200 nm increases the possibility that some of them might use the above mechanism to bind to the calcium phosphate crystals in the bone.

3.7. Encapsulation efficiency of PEI:DNAoligo in PLGA nanocapsules

Loading and encapsulation efficiency are two very important parameters in adjusting the dose and the efficacy of the drug delivery system. In the determination of encapsulation efficiency, PEI and FAM-labelled DNAoligo were used at a N/P ratio of 20 in the preparation of PLGA nanocapsules. The FI of the FAM label determined was used to calculate the amount of complex encapsulated (λ_{ex}: 494 nm, λ_{em}: 524 nm). The amount of the encapsulated complex was calculated by the calibration curve obtained from empty nanocapsule PEI:FAM labelled DNAoligo complexes (N/P 20) carrying known amounts of FAM labelled DNA oligo. The encapsulation efficiency was calculated to be 48.1 ± 1.4% and the loading was 192 ± 4 ng/mg PLGA nanocapsule.

3.8. Release of PEI:DNAoligo complex from PLGA nanocapsules

The goal of this study was to develop a system to deliver siRNA to the bone tissue and one of the important factors that influence the efficacy is the rate with which the siRNA is made

Table 2. Diameter and PDI values of empty, PEI:DNAoligo (20:1) loaded, and ELR coated PEI:DNAoligo (20:1) loaded PLGA nanocapsules.

Sample	Diameter (nm)	Polydispersity index
Empty PLGA nanocapsule	208 ± 83	0.18
PEI:DNAoligo (20:1) loaded PLGA nanocapsule	197 ± 76	0.17
ELR coated PEI:DNAoligo (20:1) loaded PLGA nanocapsule	220 ± 81	0.63

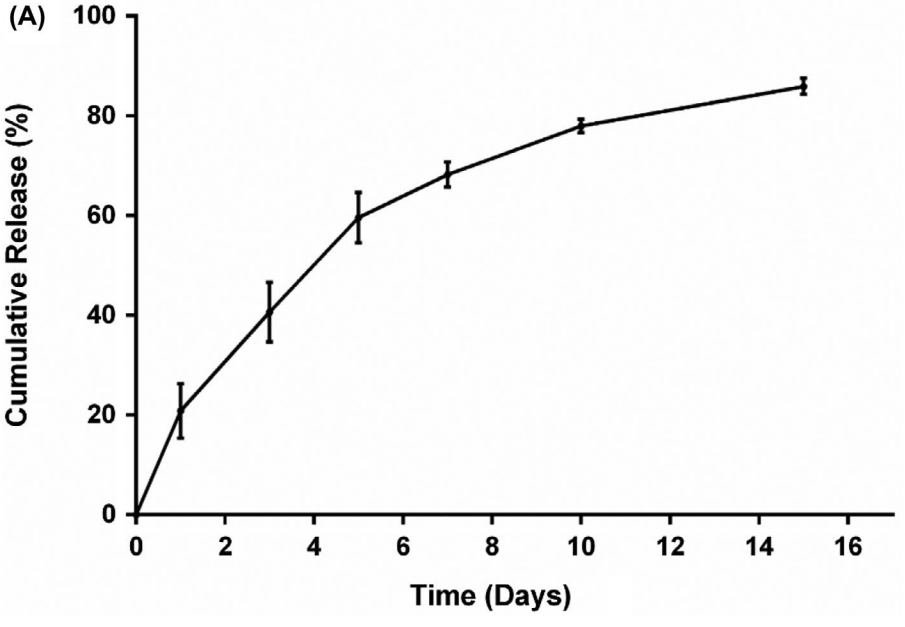

(B)

PEI:DNAoligo Complex	Release models, rate constant (k) and r^2 values					
	Zero Order		First Order		Higuchi	
	k	r^2	k	r^2	k	r^2
	8.553	0.86	0.089	0.73	0.233	0.96

Figure 9. Release of PEI: DNAoligo from PLGA nanocapsules (pH 7.4). (A) Cumulative release of PEI:DNAoligo complex from nanocapsules. (B) Release kinetics of PEI:DNAoligo complex. Quantification was done by measuring the fluorescence intensities on Days 1, 3, 5, 7, 10 and 15 ($n = 3$). Release of the complex from the nanocapsules indicated a 20% release in the first 24 h and the release rate gradually decreased according to Higuchi release kinetics.

available to the bone cells. In the studies conducted to assess the rate of release of the complex from the PLGA nanocapsules, the amount of complex remaining in the capsules was measured by using the fluorescence of the FAM-labelled DNA oligo and then deducted from the entrapped value to determine the released amount through mass balance (Figure 9). On Day 1, capsules released 20% of their content and then the released amount gradually decreased. On day 15 the cumulative release was calculated to be 80%.

4. Conclusion

The results of the present study show that ELR coated PEI:nucleic acid complex carrying nanocapsules are successfully prepared. PEI:DNAoligo complex was seen to mimic

Downloaded by [University of Alberta] at 13:21 18 September 2017

PEI:siRNA complex, and that the complex can be encapsulated in PLGA nanocapsules. The ELR coated nucleic acid carrying PLGA nanocapsules were in the size range of the fenestrations in the bone marrow endothelium indicating that the extravasation of the nanocapsules towards the ECM of bone is possible. As a result, these nanocapsules can be targeted to the HAp crystals in the extracellular matrix of bone tissue by using the recombinant polypeptide elastin like recombinamer used in this study. The delivery system designed and developed in this study can be used as a tool for siRNA delivery to bone tissue for the treatment of bone specific diseases such as osteoporosis. We are currently determining the silencing efficacy of PEI:siRNA loaded PLGA nanocapsules *in vitro*.

Acknowledgments

The authors acknowledge BIOMATEN, the Middle East Technical University Center of Excellence in Biomaterials and Tissue Engineering for the use of the facilities. Deniz Sezlev Bilecen acknowledges TUBITAK BIDEB 2211-c scholarship.

Disclosure statement

No potential conflict of interest was reported by the authors.

Funding

This study was supported by the Middle East Technical University [BAP-07-02-2012-1001-78]; EC [HEALTH-F4-2011-278557, PITN-GA-2012-317306, MSCA-ITN-2014-642687 and NMP-2014-646075]; MINECO [MAT2013-42473-R and MAT2015-68901R]; JCyL [VA244U13, VA313U14 and VA015U16]. DSB acknowledges TUBITAK BIDEB 2211-c scholarship.

References

[1] Holroyd C, Cooper C, Dennison E. Epidemiology of osteoporosis. Best Pract Res Clin Endocrinol Metab. 2008;22:671–685. Epub 2008/11/26.
[2] Kanis JA. Assessment of osteoporosis at the primary health care level. Sheffield: World Heath Organization Scientific Group Technical Report, University of Sheffield: 66. 2007.
[3] Akesson K. New approaches to pharmacological treatment of osteoporosis. Bull World Health Organ. 2003;81:657–664. Epub 2004/01/09.
[4] Das S, Crockett JC. Osteoporosis – a current view of pharmacological prevention and treatment. Drug Des Dev Ther. 2013;7:435–448. Epub 2013/06/29.
[5] Zhang Y, Dusad A, Ren K. Drug delivery strategies for treating osteoporosis. Orthopedic Muscul Sys. 2014;S2:003. doi:10.4172/2161-0533.S2-003.
[6] Fazil M, Ali A, Baboota S, et al. Exploring drug delivery systems for treating osteoporosis. Expert Opin Drug Delivery. 2013;10:1123–1136. Epub 2013/03/30.
[7] Carbone EJ, Rajpura K, Allen BN, et al. Osteotropic nanoscale drug delivery systems based on small molecule bone-targeting moieties. Nanomed Nanotechnol Biol Med. 2017;13:37–47.
[8] Miladi K, Sfarb S, Fessia H, et al. Drug carriers in osteoporosis: preparation, drug encapsulation and applications. Int J Pharm. 2013;445:181–195.
[9] Shi X, Wang Y, Ren L, et al. Enhancing alendronate release from a novel PLGA/hydroxyapatite microspheric system for bone repairing applications. Pharm Res. 2009;26:422–430.
[10] Narayanan D, Anitha A, Jayakumar R, et al. Synthesis, characterization and preliminary *in vitro* evaluation of PTH 1-34 loaded chitosan nanoparticles for osteoporosis. J Biomed Nanotechnol. 2012;8:98–106. Epub 2012/04/21.

Downloaded by [University of Alberta] at 13:21 18 September 2017

[11] Hosny KM. Alendronate sodium as enteric coated solid lipid nanoparticles; preparation, optimization, and *ın vivo* evaluation to enhance Its oral bioavailability. PLoS One. 2016; 11:e0154926.
[12] Fazil M, Hassan MQ, Baboota S, et al. Biodegradable intranasal nanoparticulate drug delivery system of risedronate sodium for osteoporosis. Drug Delivery. 2016;23:2428–2438.
[13] Elbashir SM, Harborth J, Lendeckel W, et al. Duplexes of 21-nucleotide RNAs mediate RNA interference in cultured mammalian cells. Nature. 2001;411:494–498.
[14] Liu X. Bone site-specific delivery of siRNA. J Biomed Res. 2016;30:264–271.
[15] Fahid FSJ, Zhu Q, Zhang C. Application of small ınterfering RNA for ınhibition of lipopolysaccharide-induced osteoclast formation and cytokine stimulation. J Endod. 2008;34:563–569.
[16] Wang Y, Grainger DW. siRNA knock-down of RANK signaling to control osteoclast-mediated bone resorption. Pharm Res. 2010;27:1273–1284.
[17] Choi B, Cui ZK, Kim S, et al. Glutamine-chitosan modified calcium phosphate nanoparticles for efficient siRNA delivery and osteogenic differentiation. J Mater Chem B. 2015;3:6448–6455.
[18] Wang Y, Tran KK, Shen H, et al. Selective local delivery of RANK siRNA to bone phagocytes using bone augmentation biomaterials. Biomaterials. 2012;33:8540–8547.
[19] Manaka T, Suzuki A, Takayama K, et al. Local delivery of siRNA using a biodegradable polymer application to enhance BMP-induced bone formation. Biomaterials. 2011;32:9642–9648.
[20] Wang Y, Grainger DW. Developing siRNA therapies to address osteoporosis. Ther Delivery. 2013;4:1239–1246.
[21] Shegokar R, Al Shaal L, Mishra PR. SiRNA delivery: challenges and role of carrier systems. Die Pharm – An Int J Pharm Sci. 2011;66:313–318.
[22] Zhang Y, Wei L, Miron RJ, et al. Anabolic bone formation via a site-specific bone-targeting delivery system by ınterfering with semaphorin 4d expression. J Bone Miner Res. 2015;30:286–296.
[23] Liang C, Guo B, Wu H, et al. Aptamer-functionalized lipid nanoparticles targeting osteoblasts as a novel RNA interference-based bone anabolic strategy. Nat Med. 2015;21:288–294. Epub 2015/02/11.
[24] Zhang G, Guo B, Wu H, et al. A delivery system targeting bone formation surfaces to facilitate RNAi-based anabolic therapy. Nat Med. 2012;18:307–314.
[25] Sun Y, Ye X, Cai M, et al. Osteoblast-targeting-peptide modified nanoparticle for siRNA/microRNA delivery. ACS Nano. 2016;10:5759–5768.
[26] Utsuno K, Uludag H. Thermodynamics of polyethylenimine-DNA binding and DNA condensation. Biophys J. 2010;99:201–207.
[27] Dominska M, Dykxhoorn DM. Breaking down the barriers: siRNA delivery and endosome escape. J Cell Sci. 2010;123(8):1183–1189.
[28] Hall A, Larsen AK, Parhamifar L, et al. High resolution respirometry analysis of polyethylenimine-mediated mitochondrial energy crisis and cellular stress: mitochondrial proton leak and inhibition of the electron transport system. Biochim Biophy Acta (BBA) – Bioenerg. 2013;1827:1213–1225. Epub 2013/07/16.
[29] Alshamsan A, Haddadi A, Hamdy S, et al. STAT3 silencing in dendritic cells by siRNA polyplexes encapsulated in PLGA nanoparticles for the modulation of anticancer ımmune response. Mol Pharm. 2010;7:1643–1654.
[30] Sahana DK, Mittal G, Bhardwaj V, et al. PLGA nanoparticles for oral delivery of hydrophobic drugs: ınfluence of organic solvent on nanoparticle formation and release behavior *ın vitro* and *ın vivo* using estradiol as a model drug. J Pharm Sci. 2008;97:1530–1542. Epub 2007/08/28.
[31] Gomez-Gaete C, TSAPIS N, BESNARD M, et al. Encapsulation of dexamethasone into biodegradable polymeric nanoparticles. Int J Pharm. 2007;331:153–159. Epub 2006/12/13.
[32] Kumari A, Yadav SK, Yadav SC. Biodegradable polymeric nanoparticles based drug delivery systems. Colloids Surf. B. 2010;75:1–18.
[33] Pradhan R, Poudel BK, Ramasamy T, et al. Docetaxel-loaded polylactic acid-co-glycolic acid nanoparticles: formulation, physicochemical characterization and cytotoxicity studies. J Nanosci Nanotechnol. 2013;13:5948–5956. Epub 2013/07/26.

Downloaded by [University of Alberta] at 13:21 18 September 2017

[34] Khan A, Benboubetra M, Sayyed PZ, et al. Sustained polymeric delivery of gene silencing antisense ODNs, siRNA, DNAzymes and ribozymes: *in vitro* and *in vivo* studies. J Drug Targeting. 2004;12:393–404.
[35] Zhou J, Patel TR, Fu M, et al. Octa-functional PLGA nanoparticles for targeted and efficient siRNA delivery to tumors. Biomaterials. 2012;33:583–591.
[36] Vasır JK, Labhasetwar V. Biodegradable nanoparticles for cytosolic delivery of therapeutics. Adv Drug Delivery Rev. 2007;59:718–728.
[37] Panyam J, Zhou WZ, Prabha S, et al. Rapid endo-lysosomal escape of poly(DL-lactide-co-glycolide) nanoparticles: implications for drug and gene delivery. FASEB J. 2002;16:1217–1226. Epub 2002/08/03.
[38] Makadia HH, Siegel JS. Poly Lactic-co-Glycolic Acid (PLGA) as biodegradable controlled drug delivery carrier. Polymers. 2011;3(3):1377–1397.
[39] Dang L, Liu J, Li F, et al. Targeted delivery systems for molecular therapy in skeletal disorders. Int J Mol Sci. 2016;17:428. Epub 2016/03/25.
[40] Thamake SI, Raut SL, Gryczynski Z, et al. Alendronate coated poly-lactic-co-glycolic acid (PLGA) nanoparticles for active targeting of metastatic breast cancer. Biomaterials. 2012;33:7164–7173. Epub 2012/07/17.
[41] Neale JR, Richter NB, Merten KE, et al. Bone selective effect of an estradiol conjugate with a novel tetracycline-derived bone-targeting agent. Bioorg Med Chem Lett. 2009;19:680–683. Epub 2009/01/02.
[42] Wang F, Chen L, Zhang R, et al. RGD peptide conjugated liposomal drug delivery system for enhance therapeutic efficacy in treating bone metastasis from prostate cancer. J Controlled Release. 2014;196:222–233. Epub 2014/12/03.
[43] Barbosa JS, Costa RR, Testera AM, et al. Multi-layered films containing a biomimetic stimuli-responsive recombinant protein. Nanoscale Res Lett. 2009;4:1247.
[44] Tejeda-Montes E, Smith KH, Rebollo E, et al. Bioactive membranes for bone regeneration applications: effect of physical and biomolecular signals on mesenchymal stem cell behavior. Acta Biomater. 2014;10:134–141.
[45] Yilgor P, Hasirci N, Hasirci V. Sequential BMP-2/BMP-7 delivery from polyester nanocapsules. J Biomed Mater Res A. 2010;93:528–536.
[46] Rodriguez-Cabello JC, Prieto S, Reguera J, et al. Biofunctional design of elastin-like polymers for advanced applications in nanobiotechnology. J Biomater Sci Polym Ed. 2007;18:269–286.
[47] Higuchi T. Rate of release of medicaments from ointment bases containing drugs in suspension. J Pharm Sci. 1961;50:874–875.
[48] Sze A, Erickson D, Ren L, et al. Zeta-potential measurement using the Smoluchowski equation and the slope of the current–time relationship in electroosmotic flow. J Colloid Interface Sci. 2003;261:402–410.
[49] Wagner M, Rinkenauer AC, Schallon A, et al. Opposites attract: influence of the molar mass of branched poly(ethylene imine) on biophysical characteristics of siRNA-based polyplexese. RSC Adv. 2013;3:12774–12785.
[50] Byler DM, Susi H. Examination of the secondary structure of proteins by deconvolved FTIR spectra. Biopolymers. 1986;25:469–487.
[51] Popescu MC, Vasile C, Craciunescu O. Structural analysis of some soluble elastins by means of FT-IR and 2D IR correlation spectroscopy. Biopolymers. 2010;93:1072–1084.
[52] Miller FA, Wilkins CH. Infrared spectra and characteristic frequencies of ınorganic ıons. Anal Chem. 1952;24:1253–1294.
[53] Ray S, Shard AG. Quantitative analysis of adsorbed proteins by X-ray photoelectron spectroscopy. Anal Chem. 2011;83:8659–8666. Epub 2011/10/04.
[54] Barua S, Mitragotri S. Challenges associated with penetration of nanoparticles across cell and tissue barriers: a review of current status and future prospects. Nano Today. 2014;9:223–243.

Downloaded by [University of Alberta] at 13:21 18 September 2017